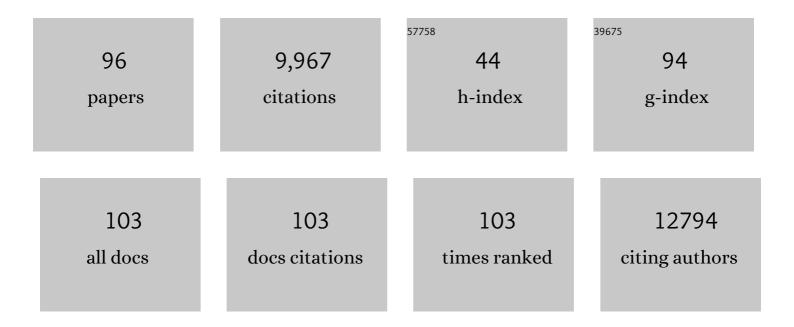
Michal Hammel

List of Publications by Year in descending order

Source: https://exaly.com/author-pdf/5081921/publications.pdf Version: 2024-02-01



#	Article	IF	CITATIONS
1	X-ray solution scattering (SAXS) combined with crystallography and computation: defining accurate macromolecular structures, conformations and assemblies in solution. Quarterly Reviews of Biophysics, 2007, 40, 191-285.	5.7	1,026
2	Structural Insights into NEDD8 Activation of Cullin-RING Ligases: Conformational Control of Conjugation. Cell, 2008, 134, 995-1006.	28.9	659
3	Robust, high-throughput solution structural analyses by small angle X-ray scattering (SAXS). Nature Methods, 2009, 6, 606-612.	19.0	610
4	XPD Helicase Structures and Activities: Insights into the Cancer and Aging Phenotypes from XPD Mutations. Cell, 2008, 133, 789-800.	28.9	593
5	Accurate SAXS Profile Computation and its Assessment by Contrast Variation Experiments. Biophysical Journal, 2013, 105, 962-974.	0.5	489
6	FoXS: a web server for rapid computation and fitting of SAXS profiles. Nucleic Acids Research, 2010, 38, W540-W544.	14.5	474
7	FoXS, FoXSDock and MultiFoXS: Single-state and multi-state structural modeling of proteins and their complexes based on SAXS profiles. Nucleic Acids Research, 2016, 44, W424-W429.	14.5	427
8	Structures of SPOP-Substrate Complexes: Insights into Molecular Architectures of BTB-Cul3 Ubiquitin Ligases. Molecular Cell, 2009, 36, 39-50.	9.7	403
9	Structure and flexibility within proteins as identified through small angle X-ray scattering. General Physiology and Biophysics, 2009, 28, 174-189.	0.9	374
10	ModBase, a database of annotated comparative protein structure models and associated resources. Nucleic Acids Research, 2014, 42, D336-D346.	14.5	275
11	Implementation and performance of SIBYLS: a dual endstation small-angle X-ray scattering and macromolecular crystallography beamline at the Advanced Light Source. Journal of Applied Crystallography, 2013, 46, 1-13.	4.5	208
12	Ku and DNA-dependent Protein Kinase Dynamic Conformations and Assembly Regulate DNA Binding and the Initial Non-homologous End Joining Complex. Journal of Biological Chemistry, 2010, 285, 1414-1423.	3.4	189
13	High-Throughput SAXS for the Characterization of Biomolecules in Solution: A Practical Approach. Methods in Molecular Biology, 2014, 1091, 245-258.	0.9	176
14	Structural insights into the interaction of IL-33 with its receptors. Proceedings of the National Academy of Sciences of the United States of America, 2013, 110, 14918-14923.	7.1	155
15	XRCC4 Protein Interactions with XRCC4-like Factor (XLF) Create an Extended Grooved Scaffold for DNA Ligation and Double Strand Break Repair. Journal of Biological Chemistry, 2011, 286, 32638-32650.	3.4	151
16	ABC ATPase signature helices in Rad50 link nucleotide state to Mre11 interface for DNA repair. Nature Structural and Molecular Biology, 2011, 18, 423-431.	8.2	149
17	A structural basis for complement inhibition by Staphylococcus aureus. Nature Immunology, 2007, 8, 430-437.	14.5	148
18	Enhancement of RAD51 recombinase activity by the tumor suppressor PALB2. Nature Structural and Molecular Biology, 2010, 17, 1255-1259.	8.2	146

#	Article	IF	CITATIONS
19	HU multimerization shift controls nucleoid compaction. Science Advances, 2016, 2, e1600650.	10.3	144
20	Atg8 Transfer from Atg7 to Atg3: A Distinctive E1-E2 Architecture and Mechanism in the Autophagy Pathway. Molecular Cell, 2011, 44, 451-461.	9.7	135
21	Mechanism of ubiquitin ligation and lysine prioritization by a HECT E3. ELife, 2013, 2, e00828.	6.0	130
22	Comprehensive macromolecular conformations mapped by quantitative SAXS analyses. Nature Methods, 2013, 10, 453-454.	19.0	112
23	Structural Basis for Marburg Virus Neutralization by a Cross-Reactive Human Antibody. Cell, 2015, 160, 904-912.	28.9	110
24	XLF Regulates Filament Architecture of the XRCC4·Ligase IV Complex. Structure, 2010, 18, 1431-1442.	3.3	104
25	Validation of macromolecular flexibility in solution by small-angle X-ray scattering (SAXS). European Biophysics Journal, 2012, 41, 789-799.	2.2	100
26	Structural insights into NHEJ: Building up an integrated picture of the dynamic DSB repair super complex, one component and interaction at a time. DNA Repair, 2014, 17, 110-120.	2.8	100
27	Macromolecular docking restrained by a small angle X-ray scattering profile. Journal of Structural Biology, 2011, 173, 461-471.	2.8	97
28	Structural Basis of Cellulosome Efficiency Explored by Small Angle X-ray Scattering. Journal of Biological Chemistry, 2005, 280, 38562-38568.	3.4	95
29	XRCC4 and XLF form long helical protein filaments suitable for DNA end protection and alignment to facilitate DNA double strand break repair. Biochemistry and Cell Biology, 2013, 91, 31-41.	2.0	91
30	Solution Structure of Human and Bovine β2-Glycoprotein I Revealed by Small-angle X-ray Scattering. Journal of Molecular Biology, 2002, 321, 85-97.	4.2	90
31	Human DNA Ligase III Recognizes DNA Ends by Dynamic Switching between Two DNA-Bound States. Biochemistry, 2010, 49, 6165-6176.	2.5	90
32	Characterization of Ehp, a Secreted Complement Inhibitory Protein from Staphylococcus aureus. Journal of Biological Chemistry, 2007, 282, 30051-30061.	3.4	84
33	Quantitative Protein Corona Composition and Dynamics on Carbon Nanotubes in Biological Environments. Angewandte Chemie - International Edition, 2020, 59, 23668-23677.	13.8	78
34	Allosteric inhibition of complement function by a staphylococcal immune evasion protein. Proceedings of the National Academy of Sciences of the United States of America, 2010, 107, 17621-17626.	7.1	77
35	Structure of a Glomulin-RBX1-CUL1 Complex: Inhibition of a RING E3 Ligase through Masking of Its E2-Binding Surface. Molecular Cell, 2012, 47, 371-382.	9.7	71
36	Modular Structure of Solubilized Human Apolipoprotein B-100. Journal of Biological Chemistry, 2006, 281, 19732-19739.	3.4	67

#	Article	IF	CITATIONS
37	Allosteric activation of the nitric oxide receptor soluble guanylate cyclase mapped by cryo-electron microscopy. ELife, 2019, 8, .	6.0	66
38	A Molecular Insight into Complement Evasion by the Staphylococcal Complement Inhibitor Protein Family. Journal of Immunology, 2009, 183, 2565-2574.	0.8	63
39	An Intrinsically Disordered APLF Links Ku, DNA-PKcs, and XRCC4-DNA Ligase IV in an Extended Flexible Non-homologous End Joining Complex. Journal of Biological Chemistry, 2016, 291, 26987-27006.	3.4	61
40	Structural Definition of a Unique Neutralization Epitope on the Receptor-Binding Domain of MERS-CoV Spike Glycoprotein. Cell Reports, 2018, 24, 441-452.	6.4	57
41	Mechanistic insights into the role of Hop2-Mnd1 in meiotic homologous DNA pairing. Nucleic Acids Research, 2014, 42, 906-917.	14.5	52
42	Structural Flexibility of the N-terminal β-Barrel Domain of 15-Lipoxygenase-1 Probed by Small Angle X-ray Scattering. Functional Consequences for Activity Regulation and Membrane Binding. Journal of Molecular Biology, 2004, 343, 917-929.	4.2	51
43	Mechanism of the Interaction of β2-Glycoprotein I with Negatively Charged Phospholipid Membranes. Biochemistry, 2001, 40, 14173-14181.	2.5	48
44	Structural Insights into the Mechanism of Formation of Cellulosomes Probed by Small Angle X-ray Scattering. Journal of Biological Chemistry, 2004, 279, 55985-55994.	3.4	48
45	Mechanism of DNA substrate recognition by the mammalian DNA repair enzyme, Polynucleotide Kinase. Nucleic Acids Research, 2009, 37, 6161-6173.	14.5	48
46	Novel bacterial clade reveals origin of form I Rubisco. Nature Plants, 2020, 6, 1158-1166.	9.3	46
47	Uncovering DNA-PKcs ancient phylogeny, unique sequence motifs and insights for human disease. Progress in Biophysics and Molecular Biology, 2021, 163, 87-108.	2.9	45
48	Mechanism of efficient double-strand break repair by a long non-coding RNA. Nucleic Acids Research, 2020, 48, 10953-10972.	14.5	43
49	Structural basis for AcrVA4 inhibition of specific CRISPR-Cas12a. ELife, 2019, 8, .	6.0	41
50	Software for the high-throughput collection of SAXS data using an enhanced <i>Blu-lce</i> / <i>DCS</i> control system. Journal of Synchrotron Radiation, 2010, 17, 774-781.	2.4	39
51	Functional Intersection of ATM and DNA-Dependent Protein Kinase Catalytic Subunit in Coding End Joining during V(D)J Recombination. Molecular and Cellular Biology, 2013, 33, 3568-3579.	2.3	39
52	Structural and functional characterization of the PNKP–XRCC4–LigIV DNA repair complex. Nucleic Acids Research, 2017, 45, 6238-6251.	14.5	39
53	Nucleoid remodeling during environmental adaptation is regulated by HU-dependent DNA bundling. Nature Communications, 2020, 11, 2905.	12.8	39
54	Transient and stabilized complexes of Nsp7, Nsp8, and Nsp12 in SARS-CoV-2 replication. Biophysical Journal, 2021, 120, 3152-3165.	0.5	39

#	Article	IF	CITATIONS
55	Structural Insights into Yeast DNA Polymerase δ by Small Angle X-ray Scattering. Journal of Molecular Biology, 2009, 394, 377-382.	4.2	38
56	Human XPG nuclease structure, assembly, and activities with insights for neurodegeneration and cancer from pathogenic mutations. Proceedings of the National Academy of Sciences of the United States of America, 2020, 117, 14127-14138.	7.1	37
57	A key interaction with RPA orients XPA in NER complexes. Nucleic Acids Research, 2020, 48, 2173-2188.	14.5	34
58	Comparison of HOCl traps with myeloperoxidase inhibitors in prevention of low density lipoprotein oxidation. BBA - Proteins and Proteomics, 2000, 1481, 109-118.	2.1	33
59	The <i>Staphylococcus aureus</i> extracellular adherence protein (Eap) adopts an elongated but structured conformation in solution. Protein Science, 2007, 16, 2605-2617.	7.6	32
60	Structural Basis for Interactions Between Contactin Family Members and Protein-tyrosine Phosphatase Receptor Type G in Neural Tissues. Journal of Biological Chemistry, 2016, 291, 21335-21349.	3.4	32
61	Modeling Structure and Dynamics of Protein Complexes with SAXS Profiles. Methods in Molecular Biology, 2018, 1764, 449-473.	0.9	31
62	Structural characterisation of nucleoside loaded low density lipoprotein as a main criterion for the applicability as drug delivery system. Chemistry and Physics of Lipids, 2003, 123, 193-207.	3.2	23
63	Flexible Tethering of ASPP Proteins Facilitates PP-1c Catalysis. Structure, 2019, 27, 1485-1496.e4.	3.3	23
64	Kinetics of tryptophan oxidation in plasma lipoproteins by myeloperoxidase-generated HOCl. FEBS Journal, 2000, 267, 4137-4143.	0.2	22
65	An atypical BRCT–BRCT interaction with the XRCC1 scaffold protein compacts human DNA Ligase IIIα within a flexible DNA repair complex. Nucleic Acids Research, 2021, 49, 306-321.	14.5	21
66	Predictive high-throughput screening of PEGylated lipids in oligonucleotide-loaded lipid nanoparticles for neuronal gene silencing. Nanoscale Advances, 2022, 4, 2107-2123.	4.6	21
67	The Immunoglobulin-like Domains 1 and 2 of the Protein Tyrosine Phosphatase LAR Adopt an Unusual Horseshoe-like Conformation. Journal of Molecular Biology, 2011, 408, 616-627.	4.2	19
68	Conformational Plasticity of the Immunoglobulin Fc Domain in Solution. Structure, 2018, 26, 1007-1014.e2.	3.3	19
69	Xâ€ray scattering reveals disordered linkers and dynamic interfaces in complexes and mechanisms for <scp>DNA</scp> doubleâ€strand break repair impacting cell and cancer biology. Protein Science, 2021, 30, 1735-1756.	7.6	19
70	Structural analysis of a new carotenoid-binding protein: the C-terminal domain homolog of the OCP. Scientific Reports, 2020, 10, 15564.	3.3	18
71	Switchable resolution in soft x-ray tomography of single cells. PLoS ONE, 2020, 15, e0227601.	2.5	18
72	Hybrid Methods Reveal Multiple Flexibly Linked DNA Polymerases within the Bacteriophage T7 Replisome. Structure, 2017, 25, 157-166.	3.3	17

5

#	Article	IF	CITATIONS
73	Quantitative Protein Corona Composition and Dynamics on Carbon Nanotubes in Biological Environments. Angewandte Chemie, 2020, 132, 23876-23885.	2.0	16
74	Rigid monoclonal antibodies improve detection of SARS-CoV-2 nucleocapsid protein. MAbs, 2021, 13, 1905978.	5.2	16
75	The structural basis for the functional comparability of factor VIII and the longâ€acting variant recombinant factor VIII Fc fusion protein. Journal of Thrombosis and Haemostasis, 2017, 15, 1167-1179.	3.8	14
76	Albumin in patients with liver disease shows an altered conformation. Communications Biology, 2021, 4, 731.	4.4	14
77	Structural basis for SHOC2 modulation of RAS signalling. Nature, 2022, 609, 400-407.	27.8	14
78	Visualizing functional dynamicity in the DNA-dependent protein kinase holoenzyme DNA-PK complex by integrating SAXS with cryo-EM. Progress in Biophysics and Molecular Biology, 2021, 163, 74-86.	2.9	13
79	Distinct Structural Features of the Peroxide Response Regulator from Group A Streptococcus Drive DNA Binding. PLoS ONE, 2014, 9, e89027.	2.5	13
80	Interdomain Communication in the Mycobacterium tuberculosis Environmental Phosphatase Rv1364c. Journal of Biological Chemistry, 2009, 284, 29828-29835.	3.4	11
81	Atypical Response Regulator ChxR from Chlamydia trachomatis Is Structurally Poised for DNA Binding. PLoS ONE, 2014, 9, e91760.	2.5	11
82	A Structural Basis for Inhibition of the Complement Initiator Protease C1r by Lyme Disease Spirochetes. Journal of Immunology, 2021, 207, 2856-2867.	0.8	11
83	Combined Solution and Crystal Methods Reveal the Electrostatic Tethers That Provide a Flexible Platform for Replication Activities in the Bacteriophage T7 Replisome. Biochemistry, 2019, 58, 4466-4479.	2.5	10
84	Hydrogen bonds are a primary driving force for <i>de novo</i> protein folding. Acta Crystallographica Section D: Structural Biology, 2017, 73, 955-969.	2.3	9
85	Functional Relevance of Interleukin-1 Receptor Inter-domain Flexibility for Cytokine Binding and Signaling. Structure, 2019, 27, 1296-1307.e5.	3.3	6
86	Direct interaction of DNA repair protein tyrosyl DNA phosphodiesterase 1 and the DNA ligase III catalytic domain is regulated by phosphorylation of its flexible N-terminus. Journal of Biological Chemistry, 2021, 297, 100921.	3.4	6
87	A monomeric mycobacteriophage immunity repressor utilizes two domains to recognize an asymmetric DNA sequence. Nature Communications, 2022, 13, .	12.8	5
88	Binding to retinoblastoma pocket domain does not alter the inter-domain flexibility of the J domain of SV40 large T antigen. Archives of Biochemistry and Biophysics, 2012, 518, 111-118.	3.0	4
89	Partition of local anesthetic heptacaine homologs between phosphatidylcholine bilayers in unilamellar liposomes and aqueous phase: UV-VIS spectrophotometry study. Die Pharmazie, 2002, 57, 499.	0.5	4
90	Crystallization and X-ray diffraction analysis of the complement component-3 (C3) inhibitory domain of Efb fromStaphylococcus aureus. Acta Crystallographica Section F: Structural Biology Communications, 2006, 62, 285-288.	0.7	3

#	Article	IF	CITATIONS
91	Heparin-mediated dimerization of follistatin. Experimental Biology and Medicine, 2021, 246, 467-482.	2.4	3
92	An improved method for the sensitive monitoring of low density lipoprotein modification by myeloperoxidase. Redox Report, 2001, 6, 257-264.	4.5	1
93	Hydrogen bonds are a primary driving force for <i>de novo</i> protein folding. Corrigendum. Acta Crystallographica Section D: Structural Biology, 2018, 74, 380-380.	2.3	1
94	Nucleoid Remodeling During Environmental Adaptation as Seen Through Soft X-ray Tomography. Microscopy and Microanalysis, 2020, 26, 2532-2533.	0.4	0
95	Scattering Methods and their Application in Colloid and Interface Science. By Otto Clatter. Elsevier, 2018. Paperback pp. 404. Price USD 225. Paperback (ISBN 9780128135808), ebook (ISBN 9780128135815) Journal of Applied Crystallography, 2019, 52, 243-244.	4.5	0
96	Structural arrangement of the VH and VL domains in the COBRAâ,,¢ T-cell engaging single-chain diabody. Antibody Therapeutics, 2022, 5, 1-10.	1.9	0